RESEARCH ARTICLE

Current reduction in a pseudo-breakup event: THEMIS observations

Z. H. Yao[1,2,3], Z. Y. Pu[3], C. J. Owen[2], S. Y. Fu[3], X. N. Chu[4], J. Liu[4], V. Angelopoulos[4], I. J. Rae[2], C. Yue[5], X.-Z. Zhou[3,4], Q.-G. Zong[3], X. Cao[1], Q. Q. Shi[6], C. Forsyth[2], and A. M. Du[1]

[1]Institute of Geology and Geophysics, Chinese Academy of Sciences, Beijing, China, [2]Mullard Space Science Laboratory, UCL, Dorking, UK, [3]School of Earth and Space Sciences, Peking University, Beijing, China, [4]Department of Earth, Planetary, and Space Sciences, University of California, Los Angeles, California, USA, [5]Department of Atmospheric and Oceanic Sciences, University of California, Los Angeles, California, USA, [6]Shandong Provincial Key Laboratory of Optical Astronomy and Solar-Terrestrial Environment, School of Space Science and Physics, Shandong University, Weihai, China

Abstract Pseudo-breakup events are thought to be generated by the same physical processes as substorms. This paper reports on the cross-tail current reduction in an isolated pseudo-breakup observed by three of the THEMIS probes (THEMIS A (THA), THEMIS D (THD), and THEMIS E (THE)) on 22 March 2010. During this pseudo-breakup, several localized auroral intensifications were seen by ground-based observatories. Using the unique spatial configuration of the three THEMIS probes, we have estimated the inertial and diamagnetic currents in the near-Earth plasma sheet associated with flow braking and diversion. We found the diamagnetic current to be the major contributor to the current reduction in this pseudo-breakup event. During flow braking, the plasma pressure was reinforced, and a weak electrojet and an auroral intensification appeared. After flow braking/diversion, the electrojet was enhanced, and a new auroral intensification was seen. The peak current intensity of the electrojet estimated from ground-based magnetometers, $\sim 0.7 \times 10^5$ A, was about 1 order of magnitude lower than that in a typical substorm. We suggest that this pseudo-breakup event involved two dynamical processes: a current-reduction associated with plasma compression ahead of the earthward flow and a current-disruption related to the flow braking/diversion. Both processes are closely connected to the fundamental interaction between fast flows, the near-Earth ambient plasma, and the magnetic field.

1. Introduction

A substorm is one of the most important energy transfer and release processes in Geospace. Although the substorm expansion phase onset has been studied for decades, its trigger mechanism (e.g., cross-tail current disruption or magnetotail reconnection (MR)) remains controversial [*Baker et al.*, 1996; *Lui*, 1996]. Greater understanding of both cross-tail current disruption and magnetotail reconnection is needed to resolve this controversy [*Ohtani*, 2001; *Cao et al.*, 2008; *Pu et al.*, 2010]. In this paper, we seek to better understand the processes leading to cross-tail current disruption.

Two models have been used to describe the causes of current disruption. In the near-Earth current disruption model [*Lui et al.*, 1992], it is suggested that current disruption is caused by plasma instabilities such as the cross-field current instability and the ballooning instability [*Roux et al.*, 1991]. The near-Earth neutral line (NENL) model gives a more complex explanation of current disruption. Fast earthward flow carrying magnetic flux ejected from the MR site is decelerated as it approaches Earth, causing a flux pileup and a magnetic dipolarization in the transition region [*Ohtani*, 2001; *Nakamura and Khotyaintsev*, 2009]. Flow braking leads to an inertial current that may contribute to current disruption [*Shiokawa et al.*, 1997]. However, the amount of inertial current is generally about 7×10^4 A, as suggested by *Shiokawa et al.* [1997]. This is insufficient to account for the amount of current disruption required for a substorm, which should be about 10^6 A [*McPherron et al.*, 1973]. Flow braking also leads to pressure gradient enhancements preceding earthward flows. These pressure gradients require the generation of field-aligned currents (FACs), which have been simulated and observed [*Birn et al.*, 1999; *Yang et al.*, 2011; *Xing et al.*, 2012; *Yao et al.*, 2012, 2013a; *Liu et al.*, 2013b]. Such field-aligned currents require reduction of the cross-tail current to conserve current continuity. Pressure gradient enhancements may also provide a free-energy source for exciting the drift ballooning-mode instability, which may also cause cross-tail current diversion [*Pu et al.*, 1999]. These processes in the NENL model may occur simultaneously, and it is difficult to distinguish the role of each in causing current

disruption. During substorm expansion, strong current disruption is essential to the formation of the substorm current wedge (SCW) [*Kepko et al.*, 2009; *Sergeev et al.*, 2014]. Weaker current disruption, on the other hand, is associated with pseudo-breakup events [*Koskinen et al.*, 1993; *Partamies et al.*, 2003].

Although similar to a substorm expansion phase onset, the disturbance in a pseudo-breakup event has amplitude below some subjective limit [*Rostoker*, 1998]. Pseudo-breakup events are suggested to be associated with disturbances within the plasma sheet that do not lead to large-scale topological changes in the magnetosphere [*Pulkkinen et al.*, 1998]. Auroras related to pseudo-breakup events are locally intensified but do not expand poleward. Pseudo-breakup events occur not only during the growth phase of substorms but also as isolated events during quiet times and at the end of substorm recovery [*Kullen et al.*, 2010]. *Rostoker* [1998] argued that disturbances in a pseudo-breakup event and in a full-scale substorm onset are caused by the same physical process. Whether a pseudo-breakup event or a substorm occurrence is ultimately controlled by the amount of solar wind energy transferred into the magnetosphere [*Kullen et al.*, 2010]. *Ohtani et al.* [2002] suggested that although fast flow localized in the *Y* direction may transport insufficient energy to cause a full-scale substorm, it may transport sufficient energy to cause a pseudo-breakup. How current disruption occurs in a pseudo-breakup event is still unclear, however.

In this paper, we report a pseudo-breakup event with the observations from three identically instrumented THEMIS probes (THEMIS A (THA), THEMIS D (THD), and THEMIS E (THE)) and ground-based magnetometer arrays on 22 March 2010. The probes were located in approximately the same *YZ* plane in GSM coordinate; THA and THE were separated mainly in the *Z* direction. The *Z* separation of THA and THE provided us with an opportunity to investigate the cross-tail current reduction/disruption during the event. To compare ground observations with observations in the magnetotail, we examined the signatures of the electrojet in the ionosphere, which can be calculated from ground-based magnetometer measurements [*Kamide and Brekke*, 1975; *Chu et al.*, 2014]. In section 2.1, we introduce the methodology used to obtain the cross-tail current evolution from in situ observations using MHD theory and Ampere's law. In sections 2.2 and 2.3, we present THEMIS ground-based and in situ observations. Our discussion and summary are in sections 3 and 4, respectively.

2. Observations

Here we report on a pseudo-breakup event which happened on 22 March 2010 using conjugate measurements from THEMIS probe instruments, All-Sky Imagers (ASIs) [*Mende et al.*, 2008], and the Canadian Array for Realtime Investigations of Magnetic Activity (CARISMA) ground magnetometers [*Mann et al.*, 2008]. At 06:40 UT, THA, THD, and THE were located at $(-11.04, -2.84, -0.58)$ R_E, $(-11.06, -2.94, -0.01)$ R_E, and $(-11.02, -2.79, -0.08)$ R_E, respectively, in GSM coordinates. Using the advantageous spatial separation of these probes, which were located approximately within the same GSM *YZ* plane, we estimate the pressure gradient in both the GSM *Y* and *Z* directions and infer the evolution of the perpendicular current, J_y, to understand the evolution of the cross-tail current disruption using the method described by *Palin et al.* [2012].

Figure 1 shows an overview of THEMIS THA, THD, and THE observations during the relevant 30 min period on 22 March 2010 fast flow event. Figure 1 (top to bottom) we plot the magnetic field, bulk velocity, and plasma pressure measured by three satellites. In this study, we mainly focus on the current evolution ahead of fast earthward flow from ~06:35 to 06:37 UT, as indicated by the pink rectangle shadow. The magnetic field B_z component dramatically increased at ~06:37 UT, indicating the onset of magnetic dipolarization or the passage of the dipolarization front. The plasma pressure was observed to increase during this time period, which suggests the plasma was compressed ahead of fast flow. During this time period, the B_x component is the dominant component of the magnetic field observed by the three satellites.

2.1. Methodology
2.1.1. Two-Dimensional Pressure Gradient Estimation
Assuming that the plasma pressure varies linearly with a constant two-dimensional gradient, $(\nabla_y P, \nabla_z P)$, within the THA, THD, and THE projections in the *YZ* plane,

$$
\begin{aligned}
P_{\text{thd}} - P_{\text{tha}} &\approx \nabla_y P \cdot (Y_{\text{thd}} - Y_{\text{tha}}) + \nabla_z P \cdot (Z_{\text{thd}} - Z_{\text{tha}}) \\
P_{\text{the}} - P_{\text{tha}} &\approx \nabla_y P \cdot (Y_{\text{the}} - Y_{\text{tha}}) + \nabla_z P \cdot (Z_{\text{the}} - Z_{\text{tha}}) \\
P_{\text{the}} - P_{\text{thd}} &\approx \nabla_y P \cdot (Y_{\text{the}} - Y_{\text{thd}}) + \nabla_z P \cdot (Z_{\text{the}} - Z_{\text{thd}})
\end{aligned}
\tag{1}
$$

where Y_{thx} and Z_{thx} are the *Y* and *Z* components of the locations of THX satellite, and P_{tha}, P_{thd}, and P_{the} are the scalar plasma pressures measured by the three probes. The two-dimensional pressure gradient can be
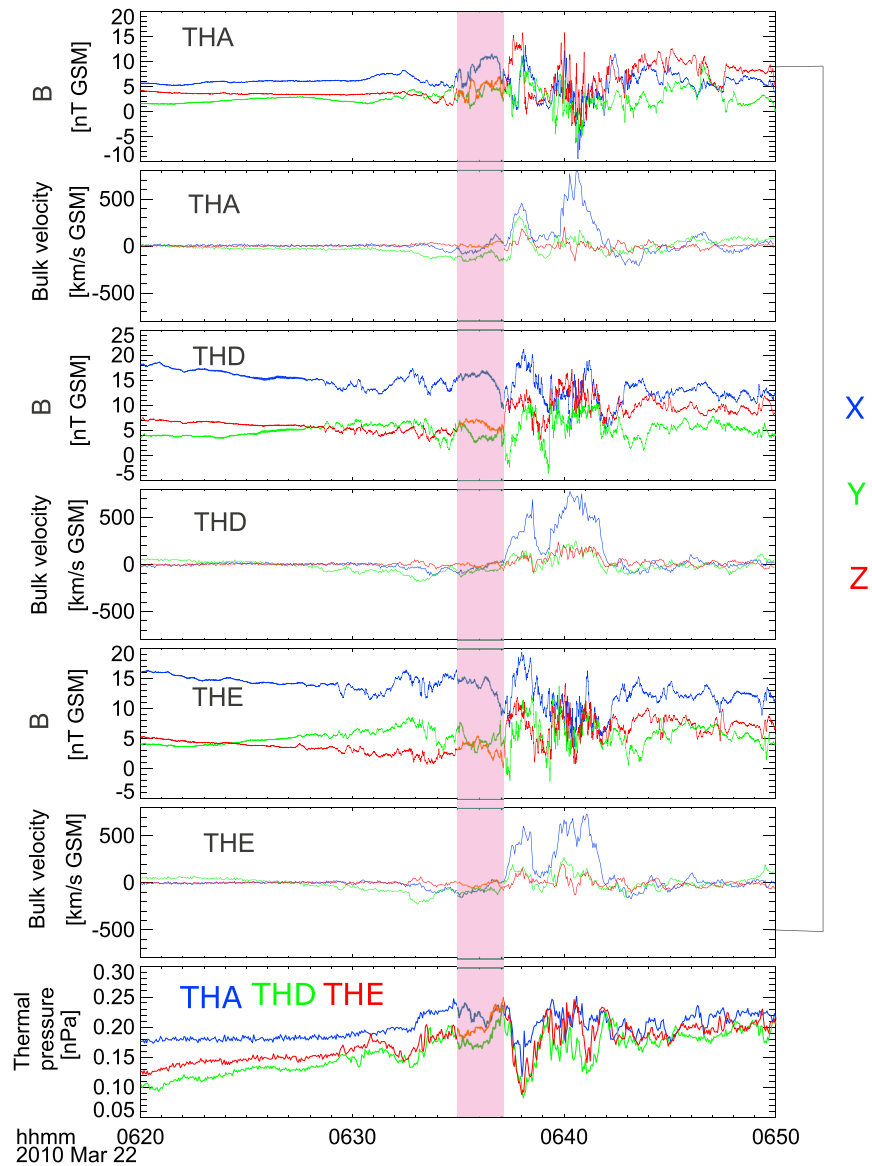
Figure 1. THEMIS A, D, and E observations between 06:20 and 06:50 UT on 22 March 2010. (the top to bottom) Magnetic field and bulk velocity of THA, THD, and THE, and plasma thermal pressure for the three probes.

obtained by solving equation (1). The method to obtain two-dimensional pressure gradient is similar as calculating the magnetic gradient using the curlometer technique [*Dunlop et al.*, 1988] but has been simplified to two dimensions.

2.1.2. Perpendicular Current From Magnetohydrodynamics Theory

The perpendicular current derived from MHD momentum equation in a one-fluid frame is

$$J_\perp = \frac{\vec{B}}{B^2} \times \rho \frac{\mathrm{d}\vec{u}}{\mathrm{d}t} + \frac{\vec{B}}{B^2} \times \nabla P \qquad (2)$$

where ρ represents the mass density, $\vec{u}$ is the bulk velocity, P represents the plasma pressure, and $\vec{J}$ and $\vec{B}$ represent the current density and magnetic field vectors, respectively. The first term on the right-hand side (RHS), usually known as the inertial term, is associated with the flow acceleration/deceleration. As we can see from the highlighted pink rectangle in Figure 1, the bulk velocity observed by all three probes is very small; we can thus ignore the inertial term in the region before the arrival of the fast flow. We will present further discussion about the inertial current associated with the flow arrival in section 3.

The second term on the RHS of equation (2), which indicates the current associated with the pressure gradient, can be rewritten as

$$\vec{J}_{\perp y} \approx \left(\frac{\vec{B} \times \nabla P}{B^2} \right)_y = -\frac{B_x (\nabla P)_z}{B^2} + \frac{B_z (\nabla P)_x}{B^2} \tag{3}$$

The second term on the RHS of equation (3), i.e., $\frac{B_z (\nabla P)_x}{B^2}$ is difficult to estimate in our study, because the pressure gradient in X direction is hard to obtain. However, since $B_x \gg B_z$ and the scale length in X direction is likely to be significantly larger than that in the Z direction, $\frac{B_z (\nabla P)_x}{B^2}$ should be much smaller than the first term on the RHS of equation (3).

In the two-fluid frame, $\nabla P = \nabla(P_i + P_e)$, so the first term in equation (3) can be rewritten as

$$\vec{J}_{\perp y} = -\frac{B_x (\nabla P_i)_z}{B^2} - \frac{B_x (\nabla P_e)_z}{B^2} \tag{4}$$

The two terms on the RHS of equation (4) represent the currents contributed by the ion and electron pressure gradients, respectively. In our calculation we use the average B_x between the two probes. The pressure gradient in the Z direction is obtained from equation (1), and we can calculate the current contributed by ions and electrons, respectively, using equation (4). The THEMIS electrostatic analyzer (ESA) [*McFadden et al.*, 2008] and solid state telescope (SST) particle detectors [*Angelopoulos*, 2008] are used to make the plasma pressure calculations.

2.1.3. Current Estimation Using Ampere's Law

We can directly calculate the current in the Y direction using Ampere's law. As suggested by *Lui* [2011], the magnetic field profile $\vec{B}_{obs}$ can be represented by the combination of a magnetic dipole $\vec{B}_{dip}$ and the magnetic field of a two-dimensional current sheet $\vec{B}_{cs}$, i.e., $\vec{B}_{obs} = \vec{B}_{dip} + \vec{B}_{cs}$.

The embedded current density between THA and THE is given by

$$\mu_0 J = \nabla \times \vec{B} = \nabla \times \left(\vec{B}_{cs} + \vec{B}_{dip} \right) = \nabla \times \vec{B}_{cs} \tag{5}$$

The zero current density from dipole magnetic field integration is applied in equation (5). Thus,

$$J_y = \frac{1}{\mu_0} \left(\frac{\partial B_x}{\partial z} - \frac{\partial B_z}{\partial x} \right) \sim \frac{1}{\mu_0} \frac{\partial B_x}{\partial z} \tag{6}$$

As suggested by *Lui* [2011], we ignored $\frac{\partial B_z}{\partial x}$ in the derivation of equation (6). The current density given by equation (6) is reliable only when the magnetic field B_x is dominant between THA and THE. For the event presented in this paper, equation (6) can be applied before flow arrival. In our study, $\frac{\partial B_x}{\partial z}$ is obtained from the measurements of THA and THE, which were separated mainly in the Z direction.

2.2. Ground-Based Observations

Figure 2 shows the auroral data and the geomagnetic field variation at the Rankin Inlet (RANK) station (at (335.7°, 72.4°) in geomagnetic coordinates). The UT time at local magnetic midnight at the station RANK is 06:25, which is in the postmidnight, but very close to the midnight meridian during the relevant observation period. We identified three independent auroral intensifications at ~06:30, ~06:32, and ~06:39 UT, as indicated by the blue arrows in Figure 2c (see also the auroral sequences in the supporting information). The variation in auroral brightness in Figure 2c is obtained by summing the total intensity in the region of interest and removing the background by subtracting the minimum total intensity between 06:00 and 06:50 UT. The H component of the magnetic field decreased from ~40 nT at ~06:34 UT to ~ −30 nT at ~06:44 UT. The electrojet estimated using an inversion technique for a current wedge is presented in Figure 2d. This technique takes ground magnetometer data as input and outputs optimal current system parameters, such as location and intensity [*Chu et al.*, 2014]. The estimated electrojet reached a peak of ~0.07 MA at around 06:44UT. During this localized auroral expansion event, aurora activity was detected by Fort Smith (FSMI), Fort Simpson (FSIM), and RANK; observations at Snap Lake (SNAP) would also appear optimal to capture this aurora brightening, but data were not available for SNAP during this time. The main auroral
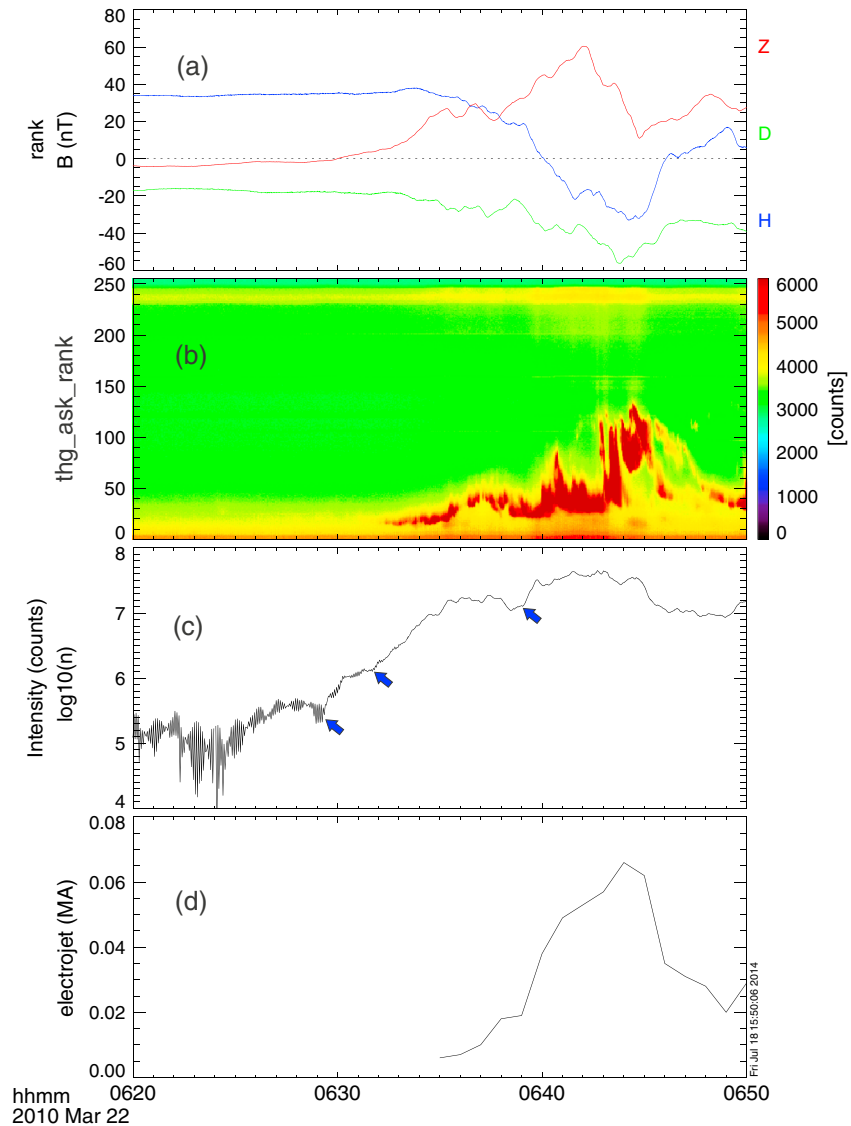
Figure 2. (a–d) Auroral keogram, magnetometer data, and the derived electrojet current from the RANK station during the 06:45 UT event on 22 March 2010.

intensifications were recorded by RANK. The reconstructed electrojet suggests that an equivalent current of $\sim 10^5$ A was flowing in the ionosphere above the RANK station at around 06:44 UT. We note that the electrojet is much weaker than in a typical substorm, which suggests that the event is a pseudo-breakup.

2.3. In Situ Observations

Figures 3a and 3b shows the pressure gradient in the *YZ* plane; the smoothed data (black lines) are obtained with a 30 s average window from the original data (red lines). The vertical blue line indicates the initiation of flow in the *Y* direction, usually considered as the consequence of flow braking and diversion, at ~06:31UT. A slight decrease in the pressure gradient in the *Z* direction, likely related to a local and weak current reduction, was observed. We suggest that this weak current reduction might relate to the auroral intensification at ~06:32UT, as indicated by the second blue arrow in Figure 2c. Figure 3c presents the current associated with the pressure gradient in *Z* direction, as described by equation (4). The blue and green lines represent the contributions from electrons and ions, respectively; the red line shows the total current. Here we have not included the contribution from $\frac{B_z(\nabla P)_x}{B^2}$, considering that the current associated with $\frac{B_z(\nabla P)_x}{B^2}$ is much smaller than the current associated with $-\frac{B_x(\nabla P)_z}{B^2}$, as discussed in section 2.1.2.
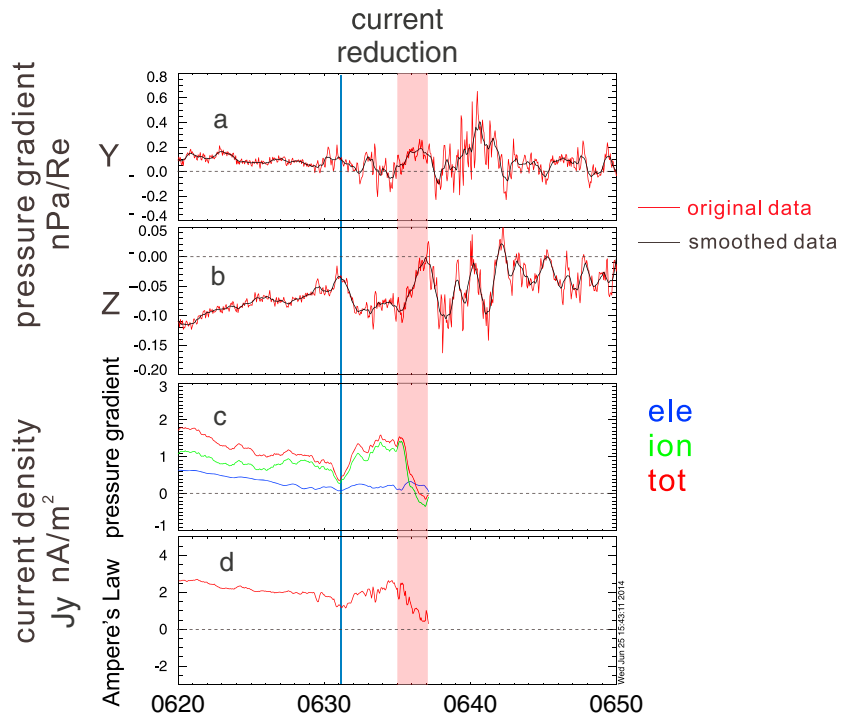
Figure 3. (a and b) The plasma pressure gradients in *Y* and *Z* direction. (c) The current derived from two-fluid MHD equation. The blue and green lines represent the current contributed by electrons and ions respectively; the red line is the total current. (d) The current derived from the Ampere's law.

From 06:35 to 06:37 UT, the average current density J_y derived from the force-balance assumption decreases from ~2 nA/m² to almost 0, as shown in Figure 3c. In Figures 3c and 3d, we only plot the derived current before 06:37 UT, because our assumptions used in equations (4) and (6) are not valid after the flow arrival and magnetic dipolarization. Clearly, the reduced currents from 06:35 to 06:37 UT are mainly carried by ions. The average current J_y given by Ampere's law decreased from ~2.5 nA/m² to almost 0, as indicated in Figure 3d. From 06:37 to 06:43 UT, $(\nabla P)_z$ fluctuated rapidly, accompanied by magnetic and electric field oscillations, which are accepted features of the cross-tail current disruption process [*Mcpherron et al.*, 1973; *Lui et al.*, 1996]. Meanwhile, $(\nabla P)_y$ was enhanced, which, according to the Vasyliunas equation [*Vasyliunas*, 1970, equation (6)] and previous studies [*Yao et al.*, 2012, 2014; *Xing et al.*, 2009], indicates field-aligned current formation. After 06:43UT, the magnetic field presented in Figure 1 was dipolarized, and the pressure gradient remained small, which imply a current sheet reconfiguration. Figures 4c and 4d show the *X* and *Y* components of both the observed electric field and the convection electric field ($-V \times B$) in despun spacecraft coordinates (DSL) [*Bonnell et al.*, 2008]. Considering that the observed electric field is not reliable in *Z* direction in DSL coordinates, we present this data in the DSL coordinate system in order to avoid a coordinate transformation which assumes E · B = 0, as adopted in many previous studies [*Lui et al.*, 1999; *Runov et al.*, 2011]. Before 06:40 UT, the observed E_X and E_Y are consistent with the convection electric field. Current density J_y variations given by Ampere's law and MHD theory are consistent during the current reduction, as shown in Figures 3c and 3d. It is noteworthy that the components of the convection electric field ($-V \times B$) are not closely consistent with those of the electric field observed in DSL coordinates after 06:38 UT, when the flow braked and diverted. In this study, the flow diversion process that is defined as the dawn-dusk flow was observed or accompanied after the earthward flow.

Fast earthward flow (~400 km/s) was observed immediately after the pressure gradient disappeared (at ~06:37 UT). We suggest that this disappearance was caused by the compressional process ahead of the earthward flow because the plasma pressure increased during compression, as shown in Figure 1 (bottom). About 2 min after the pressure gradient vanished, which implied a reduction in the cross-tail current, an auroral intensification was observed as indicated by the third blue arrow in Figure 2c. The constructed electrojet was dramatically enhanced for the third auroral intensification, as shown in Figure 2d.
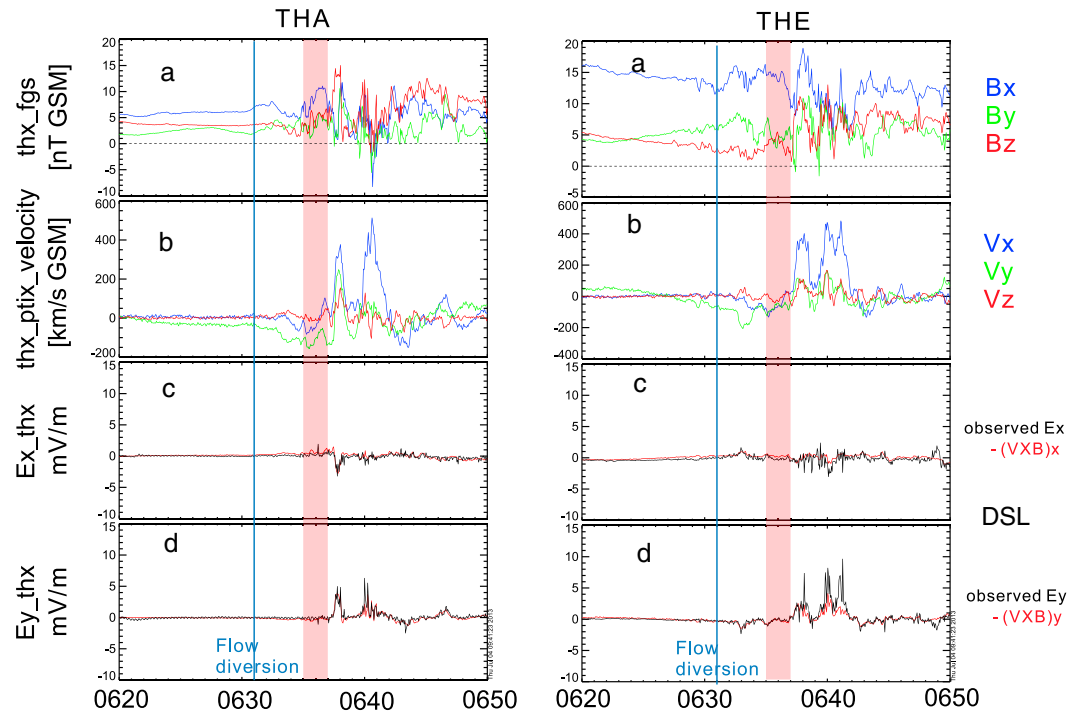
Figure 4. (a) Magnetic field components in GSM coordinates. (b) Bulk velocity components in GSM coordinate. (c and d) X and Y components of observed electric field and the convection electric field in DSL coordinates. Left (right) panels show the observations from THA (THE).

3. Discussion

In our study, we have ignored the inertial current in the compressional region before the arrival of flow. As we mentioned in section 2.1.3, the deceleration of the flow may also contribute to cross-tail current reduction [*Shiokawa et al.*, 1997]. Before the arrival of earthward fast flow, i.e., ~06:37 UT, the inertial current should be negligible. Meanwhile, the intensity of the inertial current associated with flow deceleration can be estimated, as shown by *Kepko et al.* [2001]

$$I_{inertial} \cong -\frac{1}{4} B_{ps}^{-1} \rho_{ps} V_x^2 I \tag{7}$$

where the subscript ps refers to the plasma sheet, ρ is the mass density, and I stands for the scale height (in Z direction) of braking. Applying the measured values from THA, which was located near the central plasma sheet ($B \sim 7$ nT, $n \sim 0.3$ cm^{-3}, $Vx \sim 400$ km/s and $I \sim 1$ R_E), we find $I_{inertial} \approx 0.18 \times 10^5$ A. The current density associated with pressure gradient reduction was about 2 nA/m^2. Assuming that the scale length of braking flow is ~1 R_E in both the X and Z directions, the total diverted current is about 0.7×10^5 A, very close to the estimated electrojet based on the ground-based magnetometer measurements and about half an order of magnitude higher than $I_{inertial}$. In summary, the pressure gradient vanishing is caused by flow braking, which is the main contributor to the current reduction in this pseudo-breakup event. The consistency between the diamagnetic current and the current derived from Ampere's law also confirms that the diamagnetic current dominates the current reduction process.

Three auroral intensifications were identified in this event. The second and third intensifications appear to be related to the two local current reduction at ~06:31 and 06:37 UT. The time delay between in situ observations and auroral intensifications is 1–2 min, consistent with those found in many previous studies [*Keiling et al.*, 2009; *Lui et al.*, 2010]. In this paper, we mainly concentrate on the third auroral intensification, during which two different processes could be identified, i.e., a compressional process before the arrival of the earthward fast flow and a flow braking/diversion process with frozen-in condition breakdown. For the flow braking/diversion process, it is shown that a larger duskward pressure gradient was formed, which corresponds to the occurrence of an upward FAC according to Vasyliunas equation. Since the observed flow was earthward
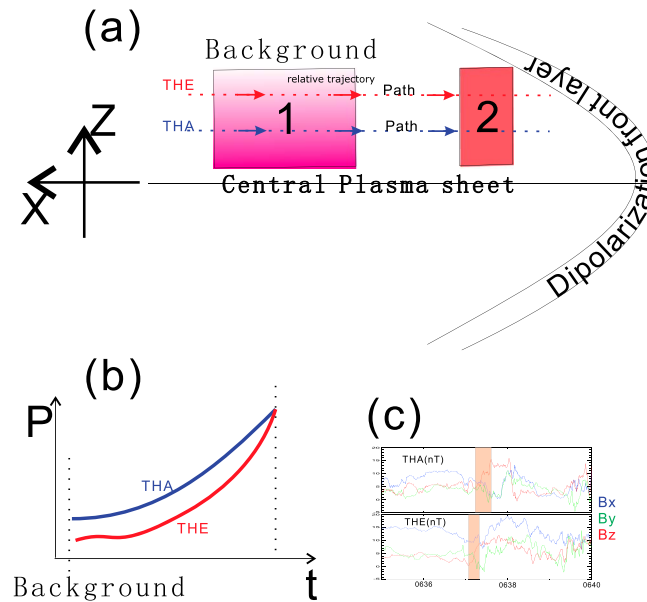
Figure 5. (a) Illustration of the current reduction process ahead of the DF. (b) Schematic description of plasma pressure variations in the inner plasma sheet and outer plasma sheet, based on the measurements at THA and THE. (c) The magnetic field observed by THA and THE.

and duskward, we suggest that the probes were located at the duskward side of the flow. The duskward pressure gradient on the duskward side of the flow is consistent with the substorm current wedgelet formation process proposed by *Yao et al.* [2012].

Near-Earth cross-tail current disruption processes are usually considered to be examples of nonfrozen-in plasma behavior [*Lui et al.*, 1999; *Lui*, 2011]. In the ~06:39 UT intensification of this pseudo-breakup event, the cross-tail current density, which was obtained from force-balance theory, was observed to be disrupted ahead of an earthward flow. Cross-tail current reductions are contributed mostly by ions, the carriers of cross-tail current [*Mitchell et al.*, 1990]. The current reduction was followed by magnetic fluctuations and dipolarization, which are also known signatures of current disruption.

The electrojet in the third intensification is ~10^5 A, an order of magnitude smaller than that in a typical substorm, i.e., ~10^6 A [*McPherron et al.*, 1973; *Kamide and Baumjohann*, 1985]. The current disruption started at the leading edge of the flow, as a sharp dipolarization front (DF) with a magnetic dip ahead of the front layer. The magnetic dip current, which is of Region 2 sense, has been studied recently [*Liu et al.*, 2013a, 2013b; *Yao et al.*, 2013b; *Sun et al.*, 2013]. Those studies presented the FAC features ahead of the DF, while this paper has studied the cross-tail current density evolution ahead of earthward flow.

Figure 5 illustrates the compressional process that we believe caused the current reduction related to the third auroral intensification. The dashed red and blue lines indicate trajectories of THE and THA relative to the DF. Before the arrival of the earthward flow, the current sheet was Harris-like (corresponded to a inward plasma pressure gradient on both sides). The plasma pressure at THE and THA was enhanced by the compressional process at the arrival of the DF and the related flow; the imbalanced ("nonuniform") compression at THE and THA resulted in decrease/disappearance of the Z component of the plasma pressure gradient. Figure 5b shows pressure variations with time at THA and THE. It is noteworthy that the DF observed at THE preceded that observed at THA (Figure 5c) by several seconds, which is also consistent with the picture presented in the cartoon. The nonuniform compressional effect ahead of the DF between the plasma sheet boundary layer and the central plasma sheet may be caused by an ion DF-reflection process, which has been reported recently in observations and particle simulations [*Zhou et al.*, 2012a, 2012b].

4. Summary

As a fundamental dynamic process in the magnetotail, the interaction between near-Earth fast flows and the ambient plasma has been considered to be an important factor for FAC formation associated with the SCW [*Forsyth et al.*, 2008; *Yao et al.*, 2012; *Birn et al.*, 2013]. This paper presents observations of a cross-tail current reduction process in the near-Earth magnetotail on 22 March 2010, which was followed by magnetic fluctuations, suggesting a current disruption occurring as part of a pseudo-breakup event. Auroral intensifications were recorded by THEMIS ASI at the RANK station at ~06:30, ~06:32, and ~06:39 UT. Our study focuses on the third intensification which was more intense than the other two. The estimated electrojet from the ground-based magnetometers is about 10^5 A, an order of magnitude smaller than that of a typical substorm. Two dynamical processes related to interaction of earthward flows with the near-Earth plasma sheet were involved in development of the pseudo-breakup. The first was nonuniform compression ahead of

the flow, which led to a local current reduction at ~06:37 UT. The second was flow diversion after the dipolarization front passed over, which yielded the azimuthal pressure gradient at ~06:41 UT and led to the formation and enhancement of FACs [*Vasyliunas*, 1970]. The peak current density of the inferred electrojet occurred at ~06:43 UT, accompanied by the major auroral intensification, which is likely to be associated with the enhancement of the azimuthal pressure gradient in the magnetotail ~2 min earlier, i.e., ~06:41 UT.

References

Angelopoulos, V. (2008), The THEMIS mission, *Space Sci. Rev.*, *141*(1), 5–34.

Baker, D. N., T. I. Pulkkinen, V. Angelopoulos, W. Baumjohann, and R. L. McPherron (1996), Neutral line model of substorms: Past results and present view, *J. Geophys. Res.*, *101*, 12,975–13,010.

Birn, J., and M. Hesse (2013), The substorm current wedge in MHD simulations, *J. Geophys. Res. Space Physics*, *118*, 3364–3376, doi:10.1002/jgra.50187.

Birn, J., M. Hesse, G. Haerendel, W. Baumjohann, and K. Shiokawa (1999), Flow braking and the substorm current wedge, *J. Geophys. Res.*, *104*, 19,895–19,903.

Bonnell, J. W., F. S. Mozer, G. T. Delory, A. J. Hull, R. E. Ergun, C. M. Cully, V. Angelopoulos, and P. R. Harvey (2008), The electric field instrument (EFI) for THEMIS, *Space Sci. Rev.*, *141*, 303–341.

Cao, X., et al. (2008), Multispacecraft and ground-based observations of substorm timing and activations: Two case studies, *J. Geophys. Res.*, *113*, A07S25, doi:10.1029/2007JA012761.

Chu, X., et al. (2014), Development and validation of inversion technique for substorm current wedge using ground magnetic field data, *J. Geophys. Res. Space Physics*, *119*, 1909–1924, doi:10.1002/2013JA019185.

Dunlop, M. W., D. J. Southwood, K.-H. Glassmeier, and F. M. Neubauer (1988), Analysis of multipoint magnetometer data, *Adv. Space Res.*, *8*(9), 273–277.

Forsyth, C., et al. (2008), Observed tail current systems associated with bursty bulk flows and auroral streamers during a period of multiple substorms, *Ann. Geophys.*, *26*, 167–184.

Kamide, Y., and W. Baumjohann (1985), Estimation of electric fields and currents from International Magnetospheric Study magnetometer data for the CDAW 6 intervals: Implications for substorm dynamics, *J. Geophys. Res.*, *90*, 1305–1317.

Kamide, Y., and A. Brekke (1975), Auroral electrojet current density deduced from the Chatanika radar and from the Alaska meridian chain of magnetic observatories, *J. Geophys. Res.*, *80*, 587–594.

Keiling, A., et al. (2009), Substorm current wedge driven by plasma flow vortices: THEMIS observations, *J. Geophys. Res.*, *114*, A00C22, doi:10.1029/2009JA014114.

Kepko, L., M. G. Kivelson, and K. Yumoto (2001), Flow bursts, braking, and Pi 2 pulsations, *J. Geophys. Res.*, *106*, 1903–1915.

Kepko, L., E. Spanswick, V. Angelopoulos, E. Donovan, J. McFadden, K.-H. Glassmeier, J. Raeder, and H. J. Singer (2009), Equatorward moving auroral signatures of a flow burst observed prior to auroral onset, *Geophys. Res. Lett.*, *36*, L24104, doi:10.1029/2009GL041476.

Koskinen, H. E. J., R. E. Lopez, R. J. Pellinen, T. I. Pulkkinen, D. N. Baker, and T. Bösinger (1993), Pseudobreakup and substorm growth-phase in the ionosphere and magnetosphere, *J. Geophys. Res.*, *98*, 5801–5813.

Kullen, A., T. Karlsson, J. A. Cumnock, and T. Sundberg (2010), Occurrence and properties of substorms associated with pseudobreakups, *J. Geophys. Res.*, *115*, A12310, doi:10.1029/2010JA015866.

Lui, A. (1996), Current disruption in the Earth's magnetosphere: Observations and models, *J. Geophys. Res.*, *101*, 13,067–13,088, doi:10.1029/96JA00079.

Lui, A. (2011), Reduction of the cross-tail current during near-Earth dipolarization with multisatellite observations, *J. Geophys. Res.*, *116*, A12239, doi:10.1029/2011JA017107.

Lui, A., R. E. Lopez, B. J. Anderson, K. Takahashi, L. J. Zanetti, R. W. McEntire, T. A. Potemra, D. M. Klumpar, E. M. Greene, and R. Strangeway (1992), Current disruptions in the near-Earth neutral sheet region, *J. Geophys. Res.*, *97*, 1461–1480.

Lui, A., K. Liou, M. Nosé, S. Ohtani, D. J. Williams, T. Mukai, K. Tsuruda, and S. Kokubun (1999), Near-Earth dipolarization: Evidence for a non-MHD process, *Geophys. Res. Lett.*, *26*, 2905–2908.

Lui, A. T. Y., E. Spanswick, E. F. Donovan, J. Liang, W. W. Liu, O. LeContel, and Q.-G. Zong (2010), A transient narrow poleward extrusion from the diffuse aurora and the concurrent magnetotail activity, *J. Geophys. Res.*, *115*, A10210, doi:10.1029/2010JA015449.

Liu, J., V. Angelopoulos, A. Runov, and X.-Z. Zhou (2013a), On the current sheets surrounding dipolarizing flux bundles in the magnetotail: The case for wedgelets, *J. Geophys. Res. Space Physics*, *118*, 2000–2020, doi:10.1002/jgra.50092.

Liu, J., V. Angelopoulos, X.-Z. Zhou, A. Runov, and Z. H. Yao (2013b), On the role of pressure and flow perturbations around dipolarizing flux bundles, *J. Geophys. Res. Space Physics*, *118*, 7104–7118, doi:10.1002/2013JA019256.

Mann, I. R., et al. (2008), The upgraded CARISMA magnetometer array in the THEMIS era, *Space Sci. Rev.*, *141*, 413–451, doi:10.1007/s11214-008-9457-6.

McFadden, J. P., C. W. Carlson, D. Larson, M. Ludlam, R. Abiad, B. Elliott, P. Turin, M. Marckwordt, and V. Angelopoulos (2008), The THEMIS ESA plasma instrument and in-flight calibration, *Space Sci. Rev.*, *141*(1), 277–302.

McPherron, R., C. T. Russell, and M. P. Aubry (1973), 9. Phenomenological model for substorms, *J. Geophys. Res.*, *78*, 3131–3149.

Mende, S. B., et al. (2008), The THEMIS array of ground-based observatories for the study of auroral substorms, *Space Sci. Rev.*, *141*, 357–387, doi:10.1007/s11214-008-9380-x.

Mitchell, D. G., D. J. Williams, C. Y. Huang, L. A. Frank, and C. T. Russell (1990), Current carriers in the near-Earth cross-tail current sheet during substorm growth phase, *Geophys. Res. Lett.*, *17*, 583–586.

Nakamura, R., and Y. Khotyaintsev (2009), Evolution of dipolarization in the near-Earth current sheet induced by earthward rapid flux transport, *Ann. Geophys.*, *27*, 1743–1754.

Ohtani, S. (2001), Substorm trigger processes in the magnetotail: Recent observations and outstanding issues, *Space Sci. Rev.*, *95*(1), 347–359.

Ohtani, S., R. Yamaguchi, H. Kawano, F. Creutzberg, J. B. Sigwarth, L. A. Frank, and T. Mukai (2002), Does the braking of the fast plasma flow trigger a substorm?: A study of the August 14, 1996, event, *Geophys. Res. Lett.*, *29*(15), 1721, doi:10.1029/2001GL013785.

Palin, L., C. Jacquey, J.-A. Sauvaud, B. Lavraud, E. Budnik, V. Angelopoulos, U. Auster, J. P. McFadden, and D. Larson (2012), Statistical analysis of dipolarizations using spacecraft closely separated along Z in the near-Earth magnetotail, *J. Geophys. Res.*, *117*, A09215, doi:10.1029/2012JA017532.

Partamies, N., O. Amm, K. Kauristie, T. I. Pulkkinen, and E. Tanskanen (2003), A pseudo-breakup observation: Localized current wedge across the postmidnight auroral oval, *J. Geophys. Res.*, *108*(A1), 1020, doi:10.1029/2002JA009276.

Pu, Z. Y., et al. (1999), Ballooning instability in the presence of a plasma flow: A synthesis of tail reconnection and current disruption models for the initiation of substorms, *J. Geophys. Res.*, *104*, 10,235–10,248.

Pu, Z. Y., et al. (2010), THEMIS observations of substorms on 26 February 2008 initiated by magnetotail reconnection, *J. Geophys. Res.*, *115*, A02212, doi:10.1029/2009JA014217.

Pulkkinen, T. I., D. N. Baker, M. Wiltberger, C. Goodrich, R. E. Lopez, and J. G. Lyon (1998), Pseudobreakup and substorm onset: Observations and MHD simulations compared, *J. Geophys. Res.*, *103*, 14,847–14,854.

Rostoker, G. (1998), On the place of the pseudo-breakup in a magnetospheric substorm, *Geophys. Res. Lett.*, *25*, 217–220.

Roux, A., S. Perraut, P. Robert, A. Morane, A. Pedersen, A. Korth, G. Kremser, B. Aparicio, D. Rodgers, and R. Pellinen (1991), Plasma sheet instability related to the westward traveling surge, *J. Geophys. Res.*, *96*, 17,697–17,714, doi:10.1029/91JA01106.

Runov, A., V. Angelopoulos, X.-Z. Zhou, X.-J. Zhang, S. Li, F. Plaschke, and J. Bonnell (2011), A THEMIS multicase study of dipolarization fronts in the magnetotail plasma sheet, *J. Geophys. Res.*, *116*, A05216, doi:10.1029/2010JA016316.

Sergeev, V. A., I. A. Chernyaev, V. Angelopoulos, A. V. Runov, and R. Nakamura (2014), Stopping flow bursts and their role in the generation of the substorm current wedge, *Geophys. Res. Lett.*, *41*, 1106–1112, doi:10.1002/2014GL059309.

Shiokawa, K., W. Baumjohann, and G. Haerendel (1997), Braking of high-speed flows in the near-Earth tail, *Geophys. Res. Lett.*, *24*, 1179–1182.

Sun, W. J., S. Y. Fu, G. K. Parks, J. Liu, Z. H. Yao, Q. Q. Shi, Q.-G. Zong, S. Y. Huang, Z. Y. Pu, and T. Xiao (2013), Field-aligned currents associated with dipolarization fronts, *Geophys. Res. Lett.*, *40*, 4503–4508, doi:10.1002/grl.50902.

Vasyliunas, V. M. (1970), Mathematical models of magnetospheric convection and its coupling to the ionosphere, in *Particles and Fields in the Magnetosphere*, edited by B. M. McCormac, pp.60–71, D. Reidel, Hingham, Mass., doi:10.1007/978-94-010-3284-1_6.

Xing, X., L. R. Lyons, V. Angelopoulos, D. Larson, J. McFadden, C. Carlson, A. Runov, and U. Auster (2009), Azimuthal plasma pressure gradient in quiet time plasma sheet, *Geophys. Res. Lett.*, *36*, L14105, doi:10.1029/2009GL038881.

Xing, X., L. R. Lyons, X.-Z. Zhou, V. Angelopoulos, E. Donovan, D. Larson, C. Carlson, and U. Auster (2012), On the formation of pre-onset azimuthal pressure gradient in the near-Earth plasma sheet, *J. Geophys. Res.*, *117*, A08224, doi:10.1029/2012JA017840.

Yang, J., F. R. Toffoletto, R. A. Wolf, and S. Sazykin (2011), RCM-E simulation of ion acceleration during an idealized plasma sheet bubble injection, *J. Geophys. Res.*, *116*, A05207, doi:10.1029/2010JA016346.

Yao, Z. H., et al. (2012), Mechanism of substorm current wedge formation: THEMIS observations, *Geophys. Res. Lett.*, *39*, L13102, doi:10.1029/2012GL052055.

Yao, Z. H., et al. (2013a), Conjugate observations of flow diversion in the magnetotail and auroral arc extension in the ionosphere, *J. Geophys. Res. Space Physics*, *118*, 4811–4816, doi:10.1002/jgra.50419.

Yao, Z. H., et al. (2013b), Current structures associated with dipolarization fronts, *J. Geophys. Res. Space Physics*, *118*, 6980–6985, doi:10.1002/2013JA019290.

Yao, Z. H., et al. (2014), Pressure gradient evolution in the near-Earth magnetotail at the arrival of BBFs, *Chin. Sci. Bull.*, *59*, doi:10.1007/s11434-014-0618-6.

Zhou, X. Z., V. Angelopoulos, A. Runov, J. Liu, and Y. S. Ge (2012a), Emergence of the active magnetotail plasma sheet boundary from transient, localized ion acceleration, *J. Geophys. Res.*, *117*, A10216, doi:10.1029/2012JA018171.

Zhou, X. Z., Y. S. Ge, V. Angelopoulos, A. Runov, J. Liang, X. Xing, J. Raeder, and Q.-G. Zong (2012b), Dipolarization fronts and associated auroral activities: 2. Acceleration of ions and their subsequent behavior, *J. Geophys. Res.*, *117*, A10227, doi:10.1029/2012JA017677.

Erratum

In the originally published version of this article, the color in Figure 1 is not correct. The error has been corrected, and this version may be considered the authoritative version of record.